Conductance in multiwall carbon nanotubes and semiconductor nanowires

J.-F. Dayen, T. L. Wade, M. Konczykowski, and J.-E. Wegrowe*
Laboratoire des Solides Irradiés, Ecole Polytechnique, CNRS-UMR 7642 and CEA/DSM/DRECAM, 91128 Palaiseau Cedex, France

X. Hoffer
Institut de Physique des Nanostructures, Ecole Polytechnique Fédérale de Lausanne, CH-1015 Lausanne, Switzerland
(Received 6 June 2005; published 8 August 2005)

Electronic transport in an ensemble of multiwall carbon nanotubes and semiconductor nanowires was compared. The nanotubes and nanowires are obtained by template synthesis and are contacted in a current perpendicular to the plane geometry by using different methods. In all cases, the nonohmic behavior of the conductance, the so-called zero-bias anomaly, shows a temperature dependence that scales with the voltage dependence. This robust scaling law describes the conductance $G(V,T)$ by a single coefficient α. A universal behavior as a function of α is found for all samples. Magnetoconductance measurements furthermore show that the conduction regime is weak localization. The observed behavior can be understood in terms of the Coulomb blockade theory, providing that a single tunnel barrier is present. This hypothetical tunnel barrier would have a resistance of the order of 2500 Ω and a typical energy of about 40 meV for all samples.

DOI: 10.1103/PhysRevB.72.073402 PACS number(s): 73.23.Hk, 73.21.Hb, 73.63.Fg, 73.63.Rt

There is intense interest in electronic transport in nanostructures in various contexts, from single electron transistors to carbon nanotubes, semiconductor nanowires, metallic nanoconstrictions, or other molecular structures. In the presence of a tunnel junction, a nonohmic behavior of the conductance G, termed zero-bias anomaly (ZBA), is generally observed at low temperature.

For carbon nanotubes (CNTs) contacted to a tunnel junction, the voltage dependence of the ZBA at low temperatures and high bias is a power law $G=G_V\,(eV)^{\alpha}$, and the temperature dependence at low bias is also a power law, with the *same power coefficient* α; $G=G_T\,(kT)^{\alpha}$ (Refs. 1–6), where e is the electronic charge and k the Boltzmann constant. Under this approximation, the conduction properties $G_{\alpha}(kT,eV)$ can then be described for each sample (at zero magnetic field) by a single scaling coefficient α, and two prefactors G_V and G_T. Beyond this approximation, a more general description is given by a scaling function f, such that $GT^{-\alpha}=f(eV/kT)$.

The scaling law is presented in the CNT literature as a manifestation of an underlying physical mechanism. In the presence of a tunnel junction, a Coulomb blockade (CB) effect is expected. In the case of an ultrasmall junction, CB is described by the environmental impedance $Z(\omega)$. [7,8] In more extended tunnel junctions with disorder, the field and electrons propagate diffusively within the electrodes, and nonperturbative methods should be used. Finally, in the case of one-dimensional (1D) systems, Luttinger liquid states are expected. In all three cases, the conductance takes an identical form [see Eq. (2) below] under a rather general hypothesis.[9–11] Furthermore, measurements of the conductivity under applied magnetic field show typical weak localization.[2,12–14]

In order to investigate the nature of scaling law, a comparative study is performed by varying the experimental parameters in the current perpendicular to the planes (CPP) geometry. Beyond CNTs, the study is enlarged to other types of nanostructures. Surprisingly, we observed that the transport properties of CNTs and Te semiconductor nanowires are statistically equivalent: it is impossible to recognize a CNT from a Te nanowire by using transport properties in the ZBA regime.

We measured two sets of samples. The first set of about 50 samples is composed of nanotubes obtained by chemical vapor deposition (CVD) on Ni or Co catalyst in a nanoporous alumina membrane (the process is described elsewhere).[6,15] The nanotubes are well separated (one nanotube per pore) and are connected perpendicularly in CPP geometry with Au, Ni, or Co contacts. The diameter of the nanotubes is calibrated by the diameter of the pore. One or a few nanotubes are contacted in parallel. The anodization techniques allow the diameter of the pores to be well controlled, from 40 down to 5 nm.[6,15] The length of the nanotube (controlled by the length of the catalyst electrodeposited inside the pores) was adjusted between about 1.5 μm down to 100 nm. The multiwall CNTs are grown inside the pores by a standard CVD technique with acetylene at 640 °C, after the electrodeposition of Ni or Co catalyst. The top contact is made by sputtering, or evaporation, after the growth of the tubes, and after exposing the samples to air. Different materials and crystallinities have been used for the top contacts.

The second set of samples is composed of single contacted tellerium semiconductors (Te) obtained by electrodeposition in nanoporous polycarbonate or alumina membranes[15] of diameters $d=40$ to 200 nm. At 200 nm, the nanowires should no longer be 1D with respect to electronic transport [because the energy separation between quantum levels $\Delta E=(\pi\hbar)^2/(2m^*d^2)$, where m^* is the effective mass, should be above the thermal energy]. With the electrodeposition technique, a single nanowire can be contacted *in situ* with a feedback loop on the intermembrane electric potential.[15] Both contacts are free of oxides, due to the chemical reduction at the Te interfaces during the electrodeposition, and due to the *in situ* contacts. The Te are contacted with Au or Ni: Au/Te/Au or Ni/Te/Ni.

The dynamical resistance measurements were performed

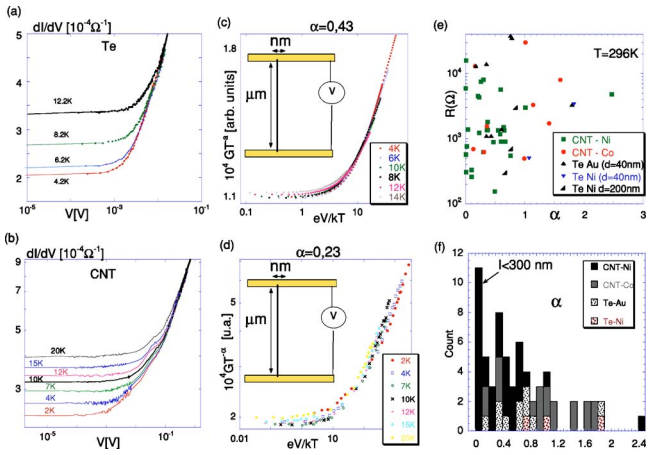

FIG. 1. Conductivity dI/dV as a function of bias voltage for different temperatures of a typical sample: (a) electrodeposited Te, (b) carbon nanotube. Scaling law of the quantity $GT^{-\alpha}$ for (c) Te and (d) CNT, with a schematic view of the samples. (e) All samples: distribution of the resistances at room temperature as a function of α and (f) histogram of scaling coefficient α.

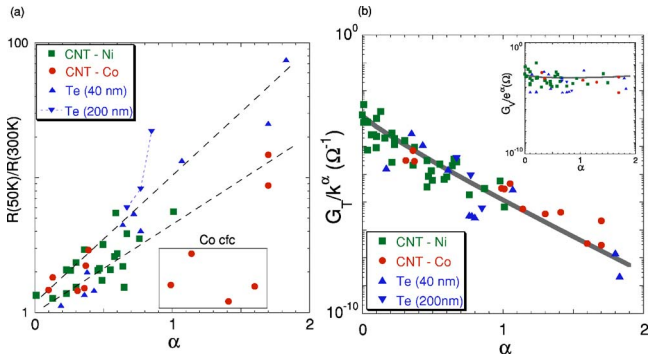

FIG. 2. (a) All samples: correlation between the ratio of the resistance at 50 K and the resistance at 300 K as a function of α. The lines are guides for the eyes. (b) Conductivity G_T/k^α for all samples (extrapolated at $T=1$ K) as a function of α. Inset: G_V/e^α (extrapolated at $V=1$ V). The data are fitted from Eq. (2) in the text, with parameters: resistance R and energy eV_0 of a tunnel junction.

with a lock-in detection bridge LR7OO (using ac current of 0.3 nA for most samples to 10 nA for low resistive samples) and a dc current. DC resistance measurements were also made with a nanovoltmeter. The temperature ranged between 4 and 200 K. A superconducting coil gives a perpendicular magnetic field, ranging between ±1.2 T. This experimental protocol allows us to measure dynamical resistance as a function of dc current amplitude, perpendicular magnetic fields, and temperature.

The typical profile of the ZBA is plotted in Fig. 1 for a Te semiconducting wire [(a) and (c)] and for a CNT sample [(b) and (d)]. The schematic view of the sample's geometry is depicted in Figs. 1(c) and 1(d). The conductance exhibits the same behavior observed for tunnel junctions. The voltage dependence of the ZBA at low temperature and high bias $G=G_V\ (eV)^\alpha$ and the temperature dependence at low bias, which is also a power law with the same power coefficient α; $G=G_T\ (kT)^\alpha$, was measured. The ZBA vanishes above 50 K, but the temperature dependence is also valid at high temperature. A more general description (which shows the deviation to the simple power-law approximation) is presented in the form: $GT^{-\alpha}=f(eV/kT)$ [Figs. 1(c) and 1(d)]. A very large majority of samples exhibit the scaling law (48 CNT over 55 with enough length[6] and 13 Te nanowires over 14). This scaling law is very robust since samples are different from the point of view of the nature of the contacts and the quality and nature of the nanowires or nanotubes. The CNTs are contacted with Ni or Co catalysts[15] on the bottom. The top of the samples is contacted either with amorphous Ni, or with highly disordered Co (mixed hcp and cfc nanocrystallites) or with single-crystalline cfc Co layer.[16] The coefficient α for Co electrodes is statistically larger than that for Ni [Fig. 1(f)].

Most of the resistances at room temperature are distributed from about 300 to 40 000 Ω [Fig. 1(e)]. There are no statistical correlations between the resistances at room temperature and the coefficient α. Figure 1(f) shows the corresponding histogram for α. The first peak near $\alpha=0$ is due to short CNTs, with a length $L\leqslant 300$ nm of the order of the thermal length (i.e., the CNTs are screened by the contacts).

There are no statistical correlations between the resistance and the length or the diameter of the CNTs (not shown). We define a ratio $\eta=R(50\text{ K})/R(300\text{ K})$ as the resistance at 50 K divided by the resistance at room temperature. The coefficient η is a measure of the contribution of the electrodes and interfaces with the exclusion of the contribution of the physical mechanism responsible for the ZBA. In other words, it gives a measure of the transparency of the barriers. The parameter η is correlated to the coefficient α [Fig. 2(a)], but the correlation depends strongly on the nature of the electrodes. A tendency is sketched by the straight lines in Fig. 2(a), and the most important deviation is seen for CNT with single-crystalline cfc Co. This shows that α is related to the transparency of the contacts, and is not exclusively defined by the states of the wires or tubes.

The most important result of this study is the unique relation existing between the prefactors (G_V, G_T), and α [Fig. 2(b)], whatever the nature of the samples. For each sample, the extrapolation at 1 K gives the conductance $G_T k^\alpha$ [plotted in Fig. 2(b)], and the extrapolation at 1 V gives the coefficient $G_V e^\alpha$ [plotted in the inset of Fig. 2(b), same scale]. All points align on the same curve.

The correlation between α and the prefactors is *a priori* not expected for two reasons. First, CB may not apply because we have no well-defined tunnel junctions. Second, if we assume a tunnel contact, the transparency of the contact would be randomly dispersed. This is indeed the case because the resistance is not correlated to α [Fig. 1(e)], and because the relation between η and α depends on the materials [see Fig. 2(a)]. Accordingly, we should expect the experimental points to be randomly dispersed in Fig. 2(b) or to be ordered according to the materials. However, the function appearing in Fig. 2(b) is a unique universality exhibited by all measured samples, providing that the scaling law is measured. The discussion of the observed relation in terms of CB [curves fitted in Fig. 2(b)] follows. In Fig. 2(b), note that the difference between the fit in the main figure and the fit in the

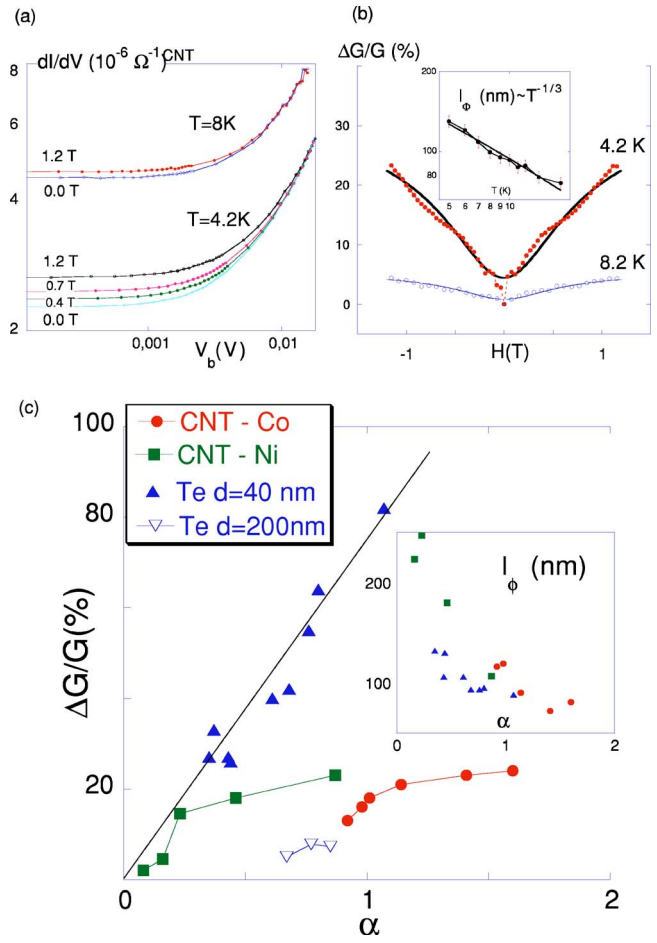

FIG. 3. (a) For a typical sample (here CNT-Co): magnetoconductance as a function of bias voltage for different-magnetic fields at 4.2 and 8 K. The field is perpendicular to the wire. (b) Magnetoconductance (same sample in %) at zero bias for different temperatures fitted by Eq. (1) to weak localization. Inset: temperature dependence of the phase-coherence length $l_\Phi \propto T^{-1/3}$. (c) All samples: correlation between magnetoconductance and coefficient α at zero bias and 4.2 K.

inset is about $(e/k)^\alpha \approx 10^{4\alpha}$, so that the two prefactors G_V and G_T are approximately equal. This means that the deviation from the approximation of the function $G_\alpha(eV,kT)$ in the two power laws is small even for intermediate regimes.

More information about the system, and especially about disorder and quantum diffusion, can be obtained by applying a magnetic field H perpendicular to the wire or tube axis.[2,13,14] Only the magnetoconductance (MC) of CNTs (1.5 μm) and Te wires (about 5 μm) of fixed length is presented. As plotted in Fig. 3(a) a positive MC is present, but depends on the bias regime, low or high. At the high bias regime, the MC is destroyed and this effect is not due to joule heating, as seen in Fig. 3(a) by comparing two temperatures. In the low bias regime, the MC exhibits all characteristics of weak localization. The MC curves at zero bias are fitted [Fig. 3(b)] with the 1D weak localization formula[2,13,14] for

$$\Delta G_{WL} = -\frac{e^2}{\pi\hbar L}(l_\Phi^{-2} + W^2/3l_m^4)^{-1/2}, \quad (1)$$

where l_Φ is the coherence length, $l_m = \sqrt{\hbar/eH}$, L is the length, and W is the radius of the wire. The fit is valid for all samples, except for the Te samples of diameter 200 nm (the large wires are no longer 1D with respect to the coherence length). The parameter l_Φ, ranged between 50 and 300 nm, is greater than the diameter of CNTs and wires, and follows the expected temperature dependence $T^{-1/3}$ [inset of Fig. 3(b)]. The decrease in the amplitude of MC with increases in the wire length and diameter has been observed. The presence of weak localization confirms the diffusive nature of the transport, and confirms the high degree of disorder. The diffusion coefficient obtained with $l_\Phi \approx 100$ nm is around $D_\Phi \approx 100$ cm^2/sec,[2,14] confirming previous results about CNTs. However, Fig. 3(c) shows that, surprisingly, the weak localization is also strongly correlated to the coefficient α. In contrast to the universal law plotted in Fig. 2(b), the relation between the MC and the coefficient α depends on the nature of the contacts for CNTs. Two different curves are present for Ni and Co contacts to CNTs. A linear relation is observed for the Te of 40-nm diam (the Au or Ni electrodes cannot be differentiated). Accordingly, α accounts also for the diffusion mechanisms, and these mechanisms depend on the nature of the interface. The coherence length is plotted as a function of α in the inset of Fig. 3(c).

We now discuss the data in terms of CB theory by assuming the presence of a tunneling junction. In the CB regime, the coefficient α is defined by the action of the electromagnetic environment on the charge carriers, or in terms of transmission lines, by the impedance Z of the circuit to which the junction is contacted. The scaling is obtained if the spectral density of electromagnetic modes $I(\omega)$ is finite at low energy down to zero-frequency modes: $\alpha = I(\omega \to 0) = Z(\omega \to 0)/(h/2e^2)$. The conductance at zero temperatures [Ref. 9, formula (19)], is given by Eq. (2) for the prefactor G_V (below). It has also been predicted that the value at finite temperature and low bias coincides [Ref. 8, Chap. 3, p. 25 (3.63)] with the expression of G_V; the bias voltage energy and the thermal energy $eV \leftrightarrow kT$ can be permutated,

$$G_T \approx G_V = \frac{1}{R}\frac{e^{-\gamma\alpha}}{\Gamma(2+\alpha)}\left(\frac{\pi\alpha}{eV_0}\right)^\alpha, \quad (2)$$

where γ is the Euler constant and $\Gamma(x)$ is the Gamma function. The resistance of the tunnel barrier is R, and the energy eV_0 is, in the case of ultrasmall tunnel junctions, the Coulomb energy $E_C = e^2/2C$, where C is the capacitance of the tunnel barrier. In a diffusive regime, the relevant energy is the Thouless energy $eV_0 = E_T = \hbar D_T/a^2$, where D_T is the diffusion constant for the charges and a the relevant length.[9,17]

As already mentioned, the power law is observed in Figs. 1(a) and 1(c). However, even assuming a hypothetical tunnel junction, it is very surprising that Eq. (2) fits the data plotted in Fig. 2(b) as a function of the coefficient α. The only fitting parameters are now the tunnel resistance R and the energy eV_0. This means that *all samples have the same tunnel barrier* (within the tolerance of one order of magnitude over

nine). The fit with Eq. (2) of the data G_T plotted as a function of α [in Fig. 2(b)] gives a tunnel resistance on the order of $R=2.5\ \mathrm{k}\Omega$, and an energy of about 40 meV, which corresponds to a capacitance of about $C=2\times10^{-18}$ F. The fit of the data G_V is less convincing, but gives, however, the same tunnel resistance and an energy of about 100 meV. The relation $G_V\approx G_T$ is confirmed within the approximation of a scaling function f composed of two power laws. For a typical length a of a few nanometers, the diffusion constant coincides with the diffusion obtained from the weak localization $D_T\approx D_\Phi\approx 100\ \mathrm{cm}^2/\mathrm{sec}$.

What is the "tunnel barrier" suggested by the experimental results, and why are the parameters of the "hypothetical tunnel barrier" deduced from the scaling law universal?[18] This problem is open, but we can already conclude that the mechanism is common to all measured samples. A common point is the geometry of the transmission line composed by the top and bottom electrodes and the membrane with the contacted nanowires (this capacitance is measured to be of the order of 1 FF/μm). The other common point, which is also common to the previous studies about MW-CNTs, is the competition between disorder and low transparency of the contacts. This would justify a more general interpretation in terms of "universal tunnel junction."

In conclusion, a comparative study of electronic transport has been performed in a current perpendicular to the plane geometry. Multiwall carbon nanotubes and electrodeposited Te nanowires have been measured. The samples are defined by a single scaling coefficient α. A universal relation is observed between α and the conductance, valid whatever the nature of the metallic electrodes, the lengths (μm range), and the diameters, ranged between 5 and 200 nm. All samples exhibit a typical weak localization behavior from which the coefficient α is also correlated. Since this result is not restricted to one-dimensional conductors, it can hardly be attributed to Luttinger liquid behavior. The application of a formula [Eq. (2)] of Coulomb blockade in a tunnel junction leads us to conclude that all happens as if a universal tunneling barrier was present for all samples.

This work was partially suported by the Swiss NSF and French DGA. We thank H. Bouchiat, S. Roche, G. Montambaux, A. Bachtold, H. Pothier, and G. L. Ingold for valuable discussions, and D. Pribat, J.-M. Padovani, and C. S. Cojocaru for their help in the CVD growth of 5 nm diam CNTs.

*Email address: jean-eric.wegrowe@polytechnique.fr

[1] M. Bockrath, D. H. Cobden, J. Lu, A. G. Rinzler, R. E. Smalley, L. Balents, and P. L. McEuen, Nature (London) **397**, 598 (1999); Z. Yao, H. W. C. Postma, L. Balents, and C. Dekker, *ibid.* **402**, 273 (1999).

[2] C. Schoenenberger, A. Bachtold, C. Strunk, J.-P. Salvetat, and L. Forro, Appl. Phys. A **A69**, 283 (1999); A. Bachtold, M. de Jonge, K. Grove-Rasmussen, P. L. McEuen, M. Buitelaaf, and C. Schönenberger, Phys. Rev. Lett. **87**, 166801 (2001).

[3] W. Yi, L. Lu, H. Hu, Z. W. Pan, and S. S. Xie, Phys. Rev. Lett. **91**, 076801 (2003).

[4] A. Kanda, K. Tsukagoshi, Y. Aoyagi, and Y. Ootuka, Phys. Rev. Lett. **92**, 036801 (2004).

[5] Th. Hunger, B. Lengeler, and J. Appenzeller, Phys. Rev. B **69**, 195406 (2004).

[6] X. Hoffer, Ch. Klinke, J.-M. Bonard, L. Gravier, and J.-E. Wegrowe, Europhys. Lett. **67**, 103 (2004); X. Hoffer, Ph.D. thesis, EPFL, Switzerland, 2004.

[7] G.-L. Ingold and Yu. V. Nazarov, in *Single Charge Tunneling*, edited by H. Grabert and M. H. Devoret, NATO Advanced Studies Institute, Series B (Plenum, New York, 1992), Vol. 294.

[8] G. Schoen, in *Quantum Transport and Dissipation*, edited by T. Dittrich, P. Haeggi, G. Ingold, B. Kramer, G. Schoen, and W. Zwerger (VCH Verlag, , 1997), chap. 3.

[9] J. Rollbühler and H. Grabert, Phys. Rev. Lett. **87**, 126804 (2001).

[10] E. G. Mishchenko, A. V. Andreev, and L. I. Glazman, Phys. Rev. Lett. **87**, 246801 (2001).

[11] R. Egger and A. O. Gogolin, Phys. Rev. Lett. **87**, 066401 (2001); Chem. Phys. Lett. **281**, 447 (2002); E. B. Sonin, Physica E (Amsterdam) **18**, 331 (2003).

[12] S. V. Zaitsev-Zotov, Yu. A. Firsov, and P. Monceau, J. Phys.: Condens. Matter **12**, L303 (2000).

[13] R. Tarkiainen, M. Ahlskog, A. Zyuzin, P. Hakonen, and M. Paalanen, Phys. Rev. B **69**, 033402 (2004); K. Liu, Ph. Avouris, R. Martel, and W. K. Hsu, *ibid.* **63**, 161404(R) (2004).

[14] B. Stojetz, Ch. Hagen, Ch. Hendlmeier, E. Ljubovic, L. Forro, and Ch. Strunk, New J. Phys. **6**, 27 (2004).

[15] T. L. Wade and J.-E. Wegrowe, Eur. Phys. J.: Appl. Phys. **29**, 3 (2005).

[16] The crystallinity of the contacts has been characterized by XRD and SQUID magnetometry.

[17] F. Pierre, H. Pothier, P. Joyez, N. O. Birge, D. Esteve, and M. H. Devoret, Phys. Rev. Lett. **86**, 1590 (2001).

[18] A metal-semiconductor junction would lead to a Schottky barrier, which can be measured in the thermoemission regime. However, since the power law holds at high temperatures, it is not compatible with an activation regime.